THE JOURNAL OF PHYSICAL CHEMISTRY B

Article

pubs.acs.org/JPCB

MRI Biosensor for Lead Detection Based on the DNAzyme-Induced Catalytic Reaction

Liguang Xu,# Honghong Yin,# Wei Ma, Libing Wang, Hua Kuang,* and Chuanlai Xu

State Key Lab of Food Science and Technology, School of Food Science and Technology, Jiangnan University, Wuxi, JiangSu 214122, People's Republic of China

Supporting Information

ABSTRACT: A MRI biosensor for sensitive and specific detection of lead ions (Pb^{2+}) was developed based on DNAzyme-induced cleavage of magnetic nanoparticles (MNPs). A low limit of detection (LOD) of 0.05 ng mL^{-1} was obtained. This biosensor has the potential to serve as a general platform for the detection of heavy metal ions.

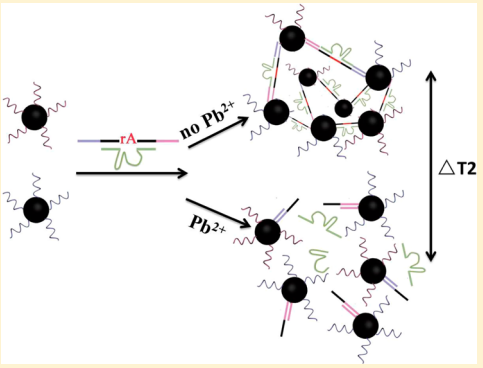

1. INTRODUCTION

Heavy metal ions are non-negligible environmental pollutants. They are biodegradable and can accumulate in the environment, resulting in contaminated food and water. Of the various heavy metal ions, contamination by Pb^{2+} is a persistent problem and a serious and long-lasting threat to the environment and human health. Even exposure to very low levels of lead can have severe effects on human health, such as neurological, reproductive, cardiovascular, and developmental disorders, particularly in children.[1−3] The most common techniques for the detection of Pb^{2+} are atomic absorption/emission spectrometry and inductively coupled plasma mass spectrometry (ICPMS).[4,5] However, these techniques are time-consuming and require sophisticated equipment and complex sample preparation. Recent advances in nanoscale sensors have enabled the development of new detection platforms aimed at more sensitive and faster detection.[6−9] However, they are not easily high-throughput for harmful elements detection. Therefore, the development of more simple, inexpensive, and high-throughput methods for Pb^{2+} detection is required.

DNAzymes are functional DNA molecules that can recognize target analytes or catalyze specific chemical and biological reactions. Metal-specific DNAzymes require specific metal ions as cofactors, and cofactor-dependent DNAzyme has provided a novel platform for the construction of DNAzyme-based sensors.[10−14] The Pb^{2+}-specific DNAzyme used in our work is the "8−17" DNAzyme obtained via in vitro selection, which can catalyze the cleavage of an RNA base in the DNA substrate in the presence of Pb^{2+}.[15−18] Numerous DNAzyme-based Pb^{2+} sensors have been developed, which mainly focus on colorimetric, dynamic light scattering (DLS), fluorescence, electrochemical, chemiluminescent, and surface-enhanced Raman scattering (SERS) methods.[19−25] However, most of the above sensors employed gold nanocrystals or fluorescent groups as an indicator. Herein, we report a novel strategy for Pb^{2+} detection using magnetic nanoparticles (MNPs).

MNPs are an important class of nanomaterials that have stimulated research interests into their fundamental properties, including superparamagnetism, high coercivity, small size effects, macroscopic quantum tunneling effects, and high magnetization.[26,27] MNPs have been widely used in physics, chemistry, medicine, biology, food safety, and environmental contamination. The main applications of MNPs are targeted drug delivery, bioseparation, diagnosis and treatment of diseases, and magnetic resonance imaging (MRI).[28−31] MRI is a nondestructive detection technology, and the MRI images of samples easily reflect detection results. In recent years, MNPs acting as contrast agents have been frequently employed in the detection of harmful elements, and fabricated MRI sensors have made a significant contribution to food safety, environmental protection, and many other fields.[32−36]

Therefore, in our work, we have taken advantage of the unique properties of MNPs and the catalytic activity of DNAzyme specific to Pb^{2+} to build a novel MRI DNAzyme sensor for the highly sensitive detection of Pb^{2+}. The organization of the MRI sensor for Pb^{2+} detection is shown in Scheme 1. The sensor contains four nucleotide sequences. The two DNA sequences of 5′ and 3′ were functionalized with an amino group (S1 and S2, respectively), which bind with carboxyl-group-modified MNPs. The 8−17 DNAzyme consists

Received: September 2, 2013
Revised: October 17, 2013
Published: October 21, 2013

Scheme 1. Scheme of the MRI Biosensor for Pb^{2+} Detection Based on DNAzyme-Induced Catalytic Reaction

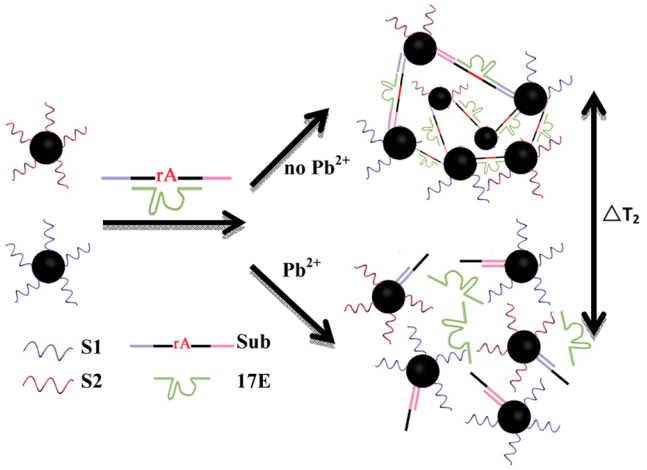

of an enzyme strand (17E) and a substrate strand (Sub). Their detailed sequences are shown in the Supporting Information. The enzyme strand has two substrate binding regions and a catalytic core, and the substrate strand has a single RNA cleavage site. At both ends of the substrate strand, 12 extra bases were added to hybridize with the two types of MNP-modified DNA. The four types of nucleotide sequences hybridized each other when they were mixed together, which resulted in aggregation of the MNPs. In the presence of Pb Pb^{2+}, the substrate strand was cleaved by the catalyst of the enzyme strand. With different concentrations of Pb^{2+}, MNPs showed different aggregation levels, and then, the spin−spin relaxation time (also known as transverse relaxation time, T_2) of the whole sample was varied. The MNP's aggregation with decreasing gradually in assembled degree can shorten the T_2 relaxation time of surrounding water just as the magnetic fields from the MNP aggregations dephase the precession of nuclear spins in water protons in the solution.

2. EXPERIMENTAL SECTION

2.1. Materials and Apparatus. 1-Ethyl-3-(3-dimethyl aminopropyl) carbodiimide hydrochloride (EDC) and *N*-hydroxy succinimide (NHS) were both obtained from Sigma-Aldrich. The Fe_3O_4 MNPs were purchased from Beijing Oneder Hightech Co., Ltd. Water used in the whole procedure was deionized and purified to 18.2 MΩ·cm resistivity at 25 °C (Millipore). All of the DNA fragments were synthesized by Shengon Biotechnology Co. Ltd. Their sequences are listed as follows:

S1:5′-NH_2-TCACAGATGAGT-3′

S2:5′-NH_2-CACGAGTTGACA-3′

17E:5′-CATCTCTTCTCCGAGCCGGTCGAA-ATAGTGAGT-3′

Sub:5′-ACTCATCTGTGAACTCACTAT(rA)-GGAAGAGATGTGTCAACTCGTG-3′

Transmission electron microscopy (TEM) images were obtained using a JEOL 2100 microscope (Japan). The size distribution of the MNPs assembly was measured by a DLS instrument (Malvern Zetasizernano, England). T_2 was determined on the Niumag-NMI20-Analyst (Shanghai Niumag Corp.), and the MRI images were obtained on the MiniMR-60 (Shanghai Niu-mag Corp.); the field intensities were 0.5 and 0.55 T, respectively.

2.2. NMR Measurement. To construct the MRI sensor to detect Pb^{2+}, 10 nM of the successfully conjugated MNPs (MNPs-S1 and MNPs-S2), 1 μM Sub, and 2 μM 17E were mixed together in 100 μL of Tris-acetate buffer (25 mM, pH 7.2, containing 100 mM NaCl) in the centrifuge tube. The sample was then heated to 70 °C and allowed to cool slowly to room temperature to promote the assembly of MNPs. The resulting DNAzyme−MNPs assembly was equilibrated for 2 min and then used as a sensor to 4 Pb^{2+}. We performed T_2 relaxation time measurements and imaging experiments using a 0.47 T NMI20-Analyst (Niumag Corp., Shanghai, China) at room temperature, as previously described. The T_2 relaxation time was measured on the centrifuge tubes using Carr−Purcell−Meiboom−Gill pulse sequences with the following parameters: echo time, 4 ms; repetition time, 6 s; the number of 180° pulses per scan, 500; the number of scans, 8.

3. RESULTS AND DISCUSSION

Fe_3O_4 MNPs with a diameter of 10.3 ± 1.6 nm were purchased from Beijing Oneder Hightech Co., Ltd. and were functionalized with carboxyl groups and showed excellent biocompatibility. The MNPs also had favorable dispersibility, as shown in Figure 1A. The carboxylic groups on the surface of the MNPs

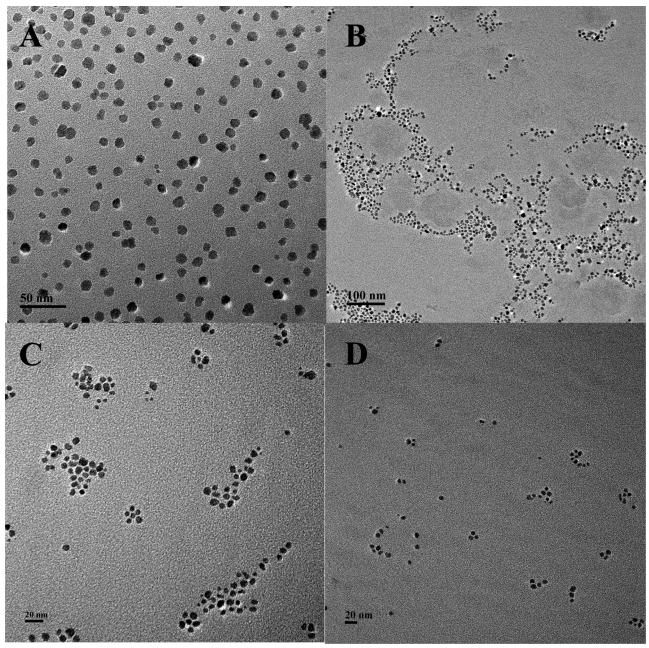

Figure 1. . Representative TEM images of MNPs and a MNPs assembly under three concentrations of Pb^{2+}. (A) Disperse MNPs, (B) MNPs assembly in the presence of 0 ng mL^{-1} of Pb^{2+}, (C) MNPs assembly in the presence of 1 ng mL^{-1} of Pb^{2+}, and (D) MNPs assembly in the presence of 10 ng mL^{-1} of Pb^{2+}.

were activated by EDC and NHS. Typically, 0.0746 mg of EDC and 0.12 mg of NHS were added to 100 μL of PBS (0.01 M sodium phosphate and 50 mM NaCl) containing 0.15 mg of Fe_3O_4 nanoparticles. After reacting for about 15 min, 10 nM MNPs were introduced into 1 μM S1 and S2, respectively, resulting in a ratio of DNA conjugated to particles of 100:1. Under gentle shaking, the coupling reaction lasted for 4 h at room temperature. Further purification by ultrafiltration was carried out to remove excess DNA using a 3000 MW cutoff membrane. Ultrafiltration was performed three times at 10000

dx.doi.org/10.1021/jp4087656 | J. Phys. Chem. B 2013, 117, 14367−14371

r/min for 5 min each time to ensure complete DNA removal. PBS was then replaced with 25 mM Tris-acetate buffer at pH 7.2.

To confirm the coupling effect between DNA oligonucleotides and Fe_3O_4 particles, DLS was adopted to determine the size variation of the Fe_3O_4 particles before and after the conjugation reaction. Compared with the original particles, the hydrodynamic size of the conjugates showed an obvious increase (Figure S1, Supporting Information). This result demonstrated that amino-modified DNA molecules were effectively coupled to carboxyl-functionalized MNPs.

The concentration of the substrate and enzyme played a critical role in the assembly of MNPs, which were optimized to improve the effect of the MRI sensor (Figures S2 and S3, detailed in the Supporting Information). The T_2 relaxation time of the MNPs assembly increased with increasing substrate concentration in the range of 100 nM to 1.5 μM and reached a plateau at 1 μM. The concentration of enzyme varied from 200 nM to 3 μM, and the T_2 values were highest at 2 μM. Therefore, to achieve efficient assembly of MNPs, 1 μM of the substrate and 2 μM of enzyme were selected for construction of the MRI sensor.

For the determination of Pb^{2+}, different concentrations of Pb^{2+} ranging from 0.1 to 20 ng mL^{-1} were added to the sensor. Determination of each sample was conducted in a 50 μL reaction system. The tube was then incubated in a water bath at 50 °C for 2 min and cooled slowly to room temperature over 2 h in the water bath. The reaction products were analyzed by MRI to reveal the variation in MNPs aggregation states. The MR images of different concentrations of Pb^{2+} are shown in Figure 2A. With an increase in Pb^{2+} concentration, the cleavage degree of DNAzyme and the dispersibility of the MNPs assembly correspondingly increased, which resulted in a decrease in the T_2 relaxation time. Thus, the brightness of the MR images gradually decreased from top to bottom. The negative control without Pb^{2+} showed the greatest level of aggregation, the T_2 relaxation time was highest, and the image was brightest.

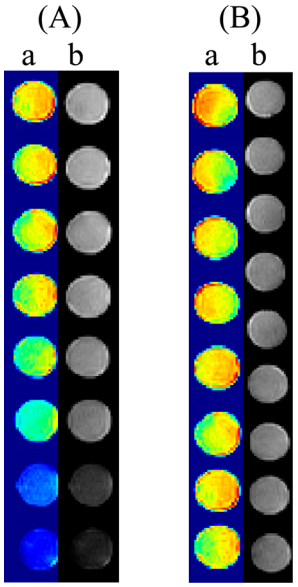

Figure 2. The T_2 values images (a) and MR image (b) of the detection. (A) The detection of Pb^{2+}; from top to bottom, the concentrations of Pb^{2+} were 0, 0.1, 0.5, 1, 2, 5, 10, and 20 ng mL^{-1}. (B) The detection of other metal ions; from top to bottom, Mn^{2+}, Zn^{2+}, Mg^{2+}, Fe^{2+}, Ca^{2+}, Hg^{2+}, and Cu^{2+}.

For the quantitative analysis of Pb^{2+}, a standard curve was established according to the T_2 values at different concentrations of Pb^{2+}, including 0.1, 0.5, 1, 2, 5, 10, and 20 ng mL^{-1}. The standard curve, which had an excellent correlation value of R^2 = 0.9939, is shown in Figure 3, and a low limit of detection (LOD) of 0.05 ng mL^{-1} was obtained.

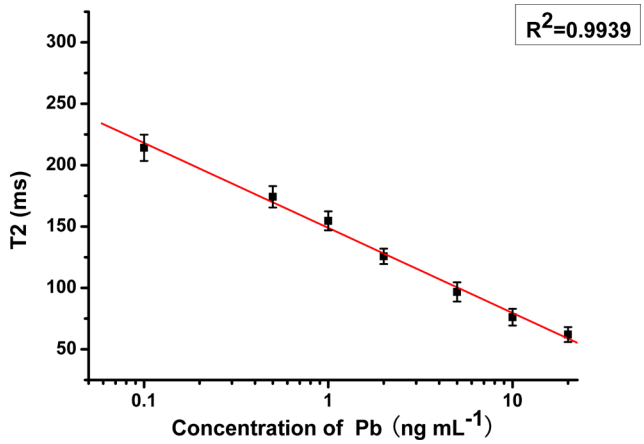

Figure 3. The standard curve of the determination of Pb^{2+}.

TEM was carried out to analyze the structure of the MNPs assembly. As shown in Figure 1B–D, at three concentrations of Pb^{2+} (0, 1, and 10 ng mL^{-1}), the typical TEM images of MNPs were measured. With an increase in Pb^{2+}, the degree of the MNPs assembly displayed a decreasing trend with cleavage of DNAzyme in the presence of more Pb^{2+}.

The selectivity of the MRI sensor was determined in the presence of various other divalent metal ions (Mn^{2+}, Zn^{2+}, Mg^{2+}, Fe^{2+}, Ca^{2+}, Hg^{2+}, and Cu^{2+}) at the concentration of 5 ng mL^{-1}. As a result, the T_2 relaxation time did not change significantly in the control without targets, and the brightness of the MR images was almost the same, as shown in Figure 2B. Therefore, these ions with the exception of Pb^{2+} ions did not have high catalytic activity toward the cleavage by 17E DNAzyme, indicating the high specificity of the designed MRI DNAzyme sensor for Pb^{2+} ion detection.

To evaluate the feasibility and reliability of the sensor, the recovery ratio of Pb^{2+} ions was determined in tap water. Following the addition of different concentrations of target Pb^{2+} (0.1, 0.2, 0.5, 1, 2, and 5 ng mL^{-1}), satisfactory recovery in the range of 92.7–97.6% was obtained (Table S1, Supporting Information). These results confirmed that this assay would be a useful test for detecting Pb^{2+} residues in real samples.

4. CONCLUSIONS

In conclusion, a highly sensitive MRI sensor was developed for the detection and quantification of Pb^{2+}. With the aid of the catalytic reaction of DNAzyme, which is specific for Pb^{2+}, the MNPs assembly was cleaved into different aggregation levels under different concentrations of Pb^{2+}. Due to the high sensitivity and resolution ratio of MRI, a low LOD of 0.05 ng mL^{-1} was observed at a Pb^{2+} range of 0.1–20 ng mL^{-1}. This MRI sensor has high-throughput, is highly sensitive and specific, can be used in real samples, and has potential in the detection of multiple metal ions.

dx.doi.org/10.1021/jp4087656 | J. Phys. Chem. B 2013, 117, 14367–14371

■ ASSOCIATED CONTENT

Supporting Information

Description of the DLS size of MNPs before and after DNA conjugation, the optimization of the substrate concentration and the enzyme concentration studied in this work (Figures S1−S3); and determination of Pb^{2+} in tap water (Table S1). This material is available free of charge via the Internet at http://pubs.acs.org.

■ AUTHOR INFORMATION

Corresponding Author

*E-mail: kuangh@jiangnan.edu.cn (H.K.).

Author Contributions

#L.X. and H.Y. contributed to this paper equally.

Notes

The authors declare no competing financial interest.

■ ACKNOWLEDGMENTS

This work is financially supported by the National Natural Science Foundation of China (21101079, 21175034, 21371081, 21301073), the Key Programs from MOST (2012BAC01B07, 2012AA06A303, 2012BAD29B04, 2012 BAK11B01, 2011BAK10B07, 2011BAK10B01, 2010AA06Z302, 2010DFB3047, 2013ZX08012-001, 2012BAK17B10, 2012BAK08B01, 2012YQ090194, 2012BAD29B05, 2013AA065501), and grants from Jiangsu Province, MOF and MOE (NCET-12-0879, BE2011626, BE2013613, BE2013611, 201310128, 201210127, 201210036, 201310135, 311002, JUSRP51308A).

■ REFERENCES

(1) Kaur, G.; Singh, H. P.; Batish, D. R.; Kohli, R. K. A Time Course Assessment of Changes in Reactive Oxygen Species Generation and Antioxidant Defense in Hydroponically Grown Wheat in Response to Lead Ions (Pb^{2+}). *Protoplasma* **2012**, *249*, 1091−1100.

(2) Guilarte, T. R.; Opler, M.; Pletnikov, M. Is Lead Exposure in Early Life an Environmental Risk Factor for Schizophrenia? Neurobiological Connections and Testable Hypotheses. *Neurotoxicology* **2012**, *33*, 560−574.

(3) Neal, A. P.; Guilarte, T. R. Molecular Neurobiology of Lead (Pb^{2+}): Effects on Synaptic Function. *Mol. Neurobiol.* **2010**, *42*, 151−160.

(4) Chen, J.; Xiao, S.; Wu, X.; Fang, K.; Liu, W. Determination of Lead in Water Samples by Graphite Furnace Atomic Absorption Spectrometry after Cloud Point Extraction. *Talanta* **2005**, *67*, 992−996.

(5) Schütz, A.; Bergdahl, I. A.; Ekholm, A.; Skerfving, S. Measurement by ICP-MS of Lead in Plasma and Whole Blood of Lead Workers and Controls. *Occup. Environ. Med.* **1996**, *53*, 736−740.

(6) Iwaniuk, D. P.; Wolf, C. A Stereodynamic Probe Providing a Chiroptical Response to Substrate-Controlled Induction of an Axially Chiral Arylacetylene Framework. *J. Am. Chem. Soc.* **2011**, *133*, 2414−2417.

(7) Fukuhara, G.; Inoue, Y. Highly Selective Oligosaccharide Sensing by a Curdlan−Polythiophene Hybrid. *J. Am. Chem. Soc.* **2010**, *133*, 768−770.

(8) Xu, Z.; Xu, L.; Liz-Marzán, L. M.; Ma, W.; Kotov, N. A.; Wang, L.; Kuang, H.; Xu, C. Sensitive Detection of Silver Ions Based on Chiroplasmonic Assemblies of Nanoparticles. *Adv. Opt. Mater.* **2013**, *1*, 626−630.

(9) Caricato, M.; Olmo, A.; Gargiulli, C.; Gattuso, G.; Pasini, D. A 'Clicked' Macrocyclic Probe Incorporating Binol as the Signalling Unit for the Chiroptical Sensing of Anions. *Tetrahedron* **2012**, *68*, 7861−7866.

(10) Niazov, T.; Pavlov, V.; Xiao, Y.; Gill, R.; Willner, I. DNAzyme-Functionalized Au Nanoparticles for the Amplified Detection of DNA or Telomerase Activity. *Nano Lett.* **2004**, *4*, 1683−1687.

(11) Hollenstein, M.; Hipolito, C.; Lam, C.; Dietrich, D.; Perrin, D. M. A Highly Selective DNAzyme Sensor for Mercuric Ions. *Angew. Chem., Int. Ed.* **2008**, *47*, 4346−4350.

(12) Lee, J. H.; Wang, Z.; Liu, J.; Lu, Y. Highly Sensitive and Selective Colorimetric Sensors for Uranyl (UO_2^{2+}): Development and Comparison of Labeled and Label-Free DNAzyme−Gold Nanoparticle Systems. *J. Am. Chem. Soc.* **2008**, *130*, 14217−14226.

(13) Breaker, R. R. DNA Enzymes. *Nat. Biotechnol.* **1997**, *15*, 427−431.

(14) Li, T.; Dong, S.; Wang, E. Label-Free Colorimetric Detection of Aqueous Mercury Ion (Hg^{2+}) Using Hg^{2+}-Modulated G-Quadruplex-Based DNAzymes. *Anal. Chem.* **2009**, *81*, 2144−2149.

(15) Breaker, R. R. In Vitro Selection of Catalytic Polynucleotides. *Chem. Rev.* **1997**, *97*, 371−390.

(16) Santoro, S. W.; Joyce, G. F. Mechanism and Utility of an RNA-Cleaving DNA Enzyme. *Biochemistry* **1998**, *37*, 13330−13342.

(17) Brown, A. K.; Li, J.; Pavot, C. M. B.; Lu, Y. A Lead-Dependent DNAzyme with a Two-Step Mechanism. *Biochemistry* **2003**, *42*, 7152−7161.

(18) Chen, J.; Zhou, X.; Zeng, L. Enzyme-Free Strip Biosensor for Amplified Detection of Pb^{2+} Based on a Catalytic DNA Circuit. *Chem. Commun.* **2013**, *49*, 984−986.

(19) Liu, J.; Lu, Y. A Colorimetric Lead Biosensor Using DNAzyme-Directed Assembly of Gold Nanoparticles. *J. Am. Chem. Soc.* **2003**, *125*, 6642−6643.

(20) Liu, J.; Lu, Y. Colorimetric Biosensors Based on DNAzyme-Assembled Gold Nanoparticles. *J. Fluoresc.* **2004**, *14*, 343−354.

(21) Liu, J.; Lu, Y. Accelerated Color Change of Gold Nanoparticles Assembled by DNAzymes for Simple and Fast Colorimetric Pb^{2+} Detection. *J. Am. Chem. Soc.* **2004**, *126*, 12298−12305.

(22) Miao, X.; Ling, L.; Shuai, X. Ultrasensitive Detection of Lead(II) with DNAzyme and Gold Nanoparticles Probes by Using a Dynamic Light Scattering Technique. *Chem. Commun.* **2011**, *47*, 4192−4194.

(23) Li, C. L.; Liu, K. T.; Lin, Y. W.; Chang, H. T. Fluorescence Detection of Lead(II) Ions through Their Induced Catalytic Activity of DNAzymes. *Anal. Chem.* **2010**, *83*, 225−230.

(24) Yang, X.; Xu, J.; Tang, X.; Liu, H.; Tian, D. A Novel Electrochemical DNAzyme Sensor for the Amplified Detection of Pb^{2+} Ions. *Chem. Commun.* **2010**, *46*, 3107−3109.

(25) Wang, Y.; Irudayaraj, J. A SERS DNAzyme Biosensor for Lead Ion Detection. *Chem. Commun.* **2011**, *47*, 4394−4396.

(26) Lu, A. H.; Salabas, E. L.; Schüth, F. Magnetic Nanoparticles: Synthesis, Protection, Functionalization, and Application. *Angew. Chem., Int. Ed.* **2007**, *46*, 1222−1244.

(27) Kodama, R. Magnetic Nanoparticles. *J. Magn. Magn. Mater.* **1999**, *200*, 359−372.

(28) Tartaj, P.; Morales, M. D. P.; Veintemillas-Verdaguer, S.; González-Carreño, T.; Serna, C. J. The Preparation of Magnetic Nanoparticles for Applications in Biomedicine. *J. Phys. D: Appl. Phys.* **2003**, *36*, R182−R197.

(29) Ito, A.; Shinkai, M.; Honda, H.; Kobayashi, T. Medical Application of Functionalized Magnetic Nanoparticles. *J. Biosci. Bioeng.* **2005**, *100*, 1−11.

(30) Lee, J. H.; Huh, Y. M.; Jun, Y.; Seo, J.; Jang, J.; Song, H. T.; Kim, S.; Cho, E. J.; Yoon, H. G.; Suh, J. S.; et al. Artificially Engineered Magnetic Nanoparticles for Ultra-Sensitive Molecular Imaging. *Nat. Med.* **2006**, *13*, 95−99.

(31) Zhou, Z. J.; Huang, D. T.; Bao, J. F.; Chen, Q. L.; Liu, G.; Chen, Z.; Chen, X. Y.; Gao, J. H. Magnetite Nanoparticles as Smart Carriers to Manipulate the Cytotoxicity of Anticancer Drugs: Magnetic Control and pH-Responsive Release. *J. Mater. Chem.* **2012**, *22*, 15717−15725.

(32) Ma, W.; Hao, C.; Ma, W.; Xing, C.; Yan, W.; Kuang, H.; Wang, L.; Xu, C. Wash-Free Magnetic Oligonucleotide Probes-Based NMR Sensor for Detecting the Hg Ion. *Chem. Commun.* **2011**, *47*, 12503−12505.

(33) Xu, Z.; Kuang, H.; Yan, W.; Hao, C.; Xing, C.; Wu, X.; Wang, L.; Xu, C. Facile and Rapid Magnetic Relaxation Switch Immunosensor for Endocrine-Disrupting Chemicals. *Biosens. Bioelectron.* **2012**, *32*, 183−187.
(34) Ma, W.; Yin, H.; Xu, L.; Wang, L.; Kuang, H.; Xu, C. A PCR Based Magnetic Assembled Sensor for Ultrasensitive DNA Detection. *Chem. Commun.* **2013**, *49*, 5369−5371.
(35) Ma, W.; Chen, W.; Qiao, R.; Liu, C.; Yang, C.; Li, Z.; Xu, D.; Peng, C.; Jin, Z.; Xu, C. Rapid and Sensitive Detection of Microcystin by Immunosensor Based on Nuclear Magnetic Resonance. *Biosens. Bioelectron.* **2009**, *25*, 240−243.
(36) Chen, Y. P.; Zou, M. Q.; Qi, C.; Xie, M. X.; Wang, D. N.; Wang, Y. F.; Xue, Q.; Li, J. F.; Chen, Y. Immunosensor Based on Magnetic Relaxation Switch and Biotin-Streptavidin System for the Detection of Kanamycin in Milk. *Biosens. Bioelectron.* **2013**, *39*, 112−117.